Sustainable Energy & Fuels

ROYAL SOCIETY OF CHEMISTRY

PAPER

View Article Online
View Journal

Cite this: DOI: 10.1039/d4se01077a

Process simulation of the integration of molecular distillation with fast pyrolysis of biomass for sustainable fuel production†

Pamela Iwube, Jun Li and Edward Brightman *

Biofuel produced from the fast pyrolysis of biomass waste can be used both to replace depleting fossil fuels and reduce environmental pollution. To improve biofuel properties, bio-oil produced by pyrolysis is fractionated using molecular distillation, which removes oxygen and converts the heavier components into lighter hydrocarbons appropriate for transportation fuels. Molecular distillation is a highly efficient separation technique widely used in industries requiring high-purity products. An increase in temperature generally enhances recovery rates but may reduce purity due to thermal degradation, while higher pressure improves purity by minimizing volatile losses but can slightly lower recovery rates. Here for the first time, we have investigated the integration of molecular distillation with fast pyrolysis of biomass as a promising route to upgrading bio-oil using process simulations to determine the optimal operating conditions that enhance product yield, purity, and recovery of specific chemicals of interest. A fast pyrolysis model was integrated with molecular distillation using ASPEN Plus software V12. The complex fast pyrolysis reactive system was analyzed and valuable insights into optimizing fast pyrolysis operating parameters and selectively isolating specific valuable chemicals was achieved. The effect of the temperature, pressure, and biomass types on the pyrolysis product yields and bio-oil compounds was also studied. Purity of up to 99.45% and recovery of 98.72% was achieved at the optimal operating conditions for levoglucosan. The molecular distillation unit selectively separated valuable bio-oil compounds of interest including levoglucosan, 4-vinyphenol, and *p*-hydroquinone. The mean free paths of the isolated compounds decreased with an increase in pressure and molecular diameter but increased slightly with temperature. By integrating biomass-fast pyrolysis with molecular distillation, there is an increase in process efficiency and selective prediction of the final product's yield. Moreover, it permits more precise isolation of chosen bio-oil compounds for different biomass waste and facilitates personalization in response to market needs.

Received 6th August 2024
Accepted 21st March 2025

DOI: 10.1039/d4se01077a

rsc.li/sustainable-energy

1 Introduction

Population growth and dwindling fossil fuel supplies have created an energy crisis around the world,[1] and conventional fossil fuel production methods release toxic gases that contribute to climate change, which has compelled researchers to seek alternative, clean, and renewable energy sources that are more sustainable. Lignocellulosic biomass, LCB, is an important energy source as it is abundant and does not interfere with food supplies.[2] For example, the yearly production of rice husks in Nigeria is estimated to be 8 700 000 tonnes. Additionally, the annual rice husk output from this paddy rice is around 1 646 980 tonnes, representing approximately 18% of the rice husk.[3] Similarly, approximately 14.5 million dry tonnes of woody biomass such as forestry residues are available in South Africa annually for bioenergy production.[4] Research and development efforts have been continuously made to effectively extract valuable products from LCB in the past decades.

Fast pyrolysis bio-oil can be upgraded to produce biofuels, chemicals, binders for asphalt, carbon materials, hydrogen, polyurethane, *etc.* Biofuels derived from biomass serves as a crucial alternative to fossil fuels and has garnered significant global interest. The bio-oil mixture often contains high water content (20–30 wt% as against 0.32 wt% for fossil fuel), highly acidic, resistant to flow, corrosiveness, low heating value (13–19 MJ kg^{-1} as against 40.63–42.39 MJ kg^{-1} for fossil fuel) and high oxygen content which hinders its use in energy generation.[5] Consequently, due to the distinct features bio-oil cannot be employed directly as a substitute for diesel and petroleum fuel in boilers, turbines, cars, airplanes, and ships.[6]

Therefore, upgrading bio-oil is thus necessary to improve its fuel properties for its practical application. Amongst the bio-oil

Department of Chemical and Process Engineering, University of Strathclyde, 75 Montrose Street, Glasgow G1 1XL, UK. E-mail: pamela.iwube@strath.ac.uk; jun.li@strath.ac.uk; edward.brightman@strath.ac.uk

† Electronic supplementary information (ESI) available. See DOI: https://doi.org/10.1039/d4se01077a

upgrading technologies, hydrodeoxygenation (HDO) is a type of catalytic pyrolysis process that eliminates the oxygen under high hydrogen pressure with a catalyst thereby increasing the thermal stability and heating value of the bio-oil. However, hydrodeoxygenation is faced with the challenge of cost due to the use of metal-oxide catalyst and their fast deactivation induced by coking, as well as the requirements for externally added hydrogen.[7] Alternatively, the use of pyrolysis-derived bio-oil as a source of chemicals can potentially avoid the costly process of hydrodeoxygenation for removing the substantial amount of oxygen in bio-oil. Oxygen-containing chemical stocks are mostly produced from fossil fuels by oxidation or hydration of olefins to add oxygen-containing functional groups.

In contrast, these functional groups already exist in bio-oil. Previous and emerging research has identified over 400 compounds that could be derived from bio-oil obtained from the pyrolysis of LCB. These compounds belong to several groups of platform chemicals and intermediate products such as convertible sugars, alcohols, acids, aldehydes, esters, furans, phenols, and other useful products of organic origin which can serve as substitutes to their fossil-derived counterparts. However, the complexity of the bio-oil mixture makes the conventional distillation methods such as steam, flash, vacuum, and atmospheric distillations inadequate as they often lead to coking and polymerization problems.

Molecular distillation (MD) also short-path distillation is a high-efficiency separation technology that have been used in the recovery and purification of thermally unstable compounds. Molecular distillation operates at relatively low temperatures (around 130 °C), thus avoiding excessive thermal degradation and coking issues common in bio-oil processing. It allows efficient fractionation of bio-oil into distinct fractions based on molecular weight and boiling points, enabling targeted upgrading strategies for each fraction. The light fractions containing reactive acids and ketones can be selectively removed, improving the stability of the remaining fractions. Molecular distillation leverages the concept of mean free path under high vacuum conditions so that molecules travel from the evaporation surface to the condenser with minimal collisions, enabling rapid separation. In contrast, traditional distillation primarily depends on differences in boiling points and relies on vapor–liquid equilibrium established over longer residence times. Currently, molecular distillation is widely used in research areas such as the production of fish oil, high concentrations of monoglyceride, fine chemicals, grease, pharmaceuticals, food processing, and concentrating organic chemicals.

Seifollahi *et al.*[8] applied short-path molecular distillation (SPMD) to deacidify lampante olive oil, reducing free fatty acids from 10.11% to 1.42%. However, economic feasibility, environmental impact, or byproduct valorization remain unaddressed. Kang *et al.*[9] performed double molecular distillation to fractionate Kushui Rose essential oil, revealing differences in aroma and biological activities among fractions. Though, quantitative data and a discussion on industrial feasibility were not included. Sagili *et al.*[10] optimized wiped-film short-path molecular distillation for cannabinoid recovery from cannabis at their chosen optimal conditions.[11] combined supercritical CO_2 extraction with MD to extract and separate *Dendranthema indicum* essential oil. Despite high antioxidant activities, separation yields were low.

Modelling tools have also been applied in molecular distillation investigations. Deng *et al.*[12] applied MD for dehydrating tetramethylammonium hydroxide. Their model showed reliability, but discrepancies in temperature simulations and lower processing capacity at optimal conditions were downsides. Similarly, Ketenoglu and Tekin [13] simulated MD of olive pomace oil deodorizer distillate, achieving close matches between experimental and simulated oleic acid concentrations. However, they tested a limited range of conditions. Idárraga-Vélez *et al.*[14] studied MD modeling, highlighting high-concentration achievements but noting varied feed flow rates and temperatures complicate industrial reproducibility. Li *et al.*[15] reviewed molecular distillation technology, praising its low-temperature operation, high separation efficiency, and environmental friendliness. The disadvantages include high equipment costs, small production capacity, and lack of theoretical research.

Overall, the molecular distillation technique currently faces the following challenges: economic feasibility and cost–benefit analysis, including equipment investment and operating costs, scalability, and industrial applicability, considering limitations in production capacity, energy consumption optimization, and potential energy savings, environmental impact assessment and sustainability analysis, comprehensive theoretical research and key data for optimal process design, trade-off analysis between process parameters (*e.g.*, feed flow rate, temperature) and desired outcomes (yield, efficiency, distillation time), long-term stability and quality assessment of distilled products, sensory evaluation for products like essential oils and edible oils, refinement of simulation models to capture non-equilibrium aspects of molecular distillation better. Additionally, achieving well-defined fractions enriched in specific compounds and developing economically viable upgrading pathways for each fraction remains a challenge. Overall, the knowledge of molecular distillation has been limited to the separation of the bio-oil compounds into light, middle, and heavy fractions. There is no focus on the extraction of specific valuable chemicals as illustrated by Wang.[16]

This study evaluates a bio-oil upgrading pathway using molecular distillation for the separation of specific bio-oil compounds for valuable chemical production. This work can serve as a framework for predicting bio-oil compounds due to changes in feedstock characteristics, as well as becoming an excellent platform for optimization studies.

2 Methodology

2.1 Model development

In this study, ASPEN Plus software (V12) was used to develop the pyrolysis model for rice husk and forestry residue biomass. The rice husk and forestry residues chosen for this study were obtained from the experimental study of Heo *et al.*[17] and van Schalkwyk *et al.*[18] Table 1 shows the ultimate and proximate analysis of rice husk and forestry residues biomass feedstocks.

Table 1 Experimental data for the ultimate and proximate analysis of rice husk and forestry residues biomass feedstocks

Components	Rice husk[17]	Forestry residues[18]
Ultimate analysis (wt%)		
Carbon	53.5	48.0
Hydrogen	7.00	6.36
Nitrogen	1.40	0.12
Oxygen	38.1	45.46
Sulphur	0	0.06
Proximate analysis (wt%)		
Moisture	9.30	8.280
Volatile matter	11.40	15.06
Fixed carbon	78.80	75.71
Ash	0.50	0.95

2.2 Pyrolysis model

The ASPEN Plus V12 pyrolysis simulation model is a steady-state, isothermal model that makes use of a sequential-modular calculation technique. Time-dependent functions like heating rate and residence time cannot be directly studied because the model is not transient but the model could be exported to ASPEN Plus Dynamics, a different but related software program, to be used for proper time investigations. The particle size distribution of the feedstock was assumed to not significantly affect the amount of energy recovered from the biomass. In other words, the simulation did not include a model for the biomass particle size. All the biomass moisture is visible as either water content in the bio-oil or minute amounts of water vapor in the synthesis gas that was produced. All sulphur in the feedstock is considered organic sulphur. Only solids are present in the char. Excluding ash, which is regarded as inert, all components participate in the chemical reaction. In the ASPEN Plus, different model blocks are specified as shown in Table 2.

The flowsheet shown in Fig. 1 illustrates the biomass-fast pyrolysis process using a non-catalytic RYield reactor, char combustor with quenching and recycling as well as condensation of the pyrolysis vapor to produce bio-oil. It is divided into five major processes which include the char combustor, riser reactor, recycle compressor, quench loop, and molecular distillation unit biomass and hot sand are added to the bottom of a vertical riser reactor. The quick heating of biomass particles to about 500 °C produces non-consensual gases and vapors of oxygenated hydrocarbons as the solids are transported up the riser by a fluidizing gas. Solid char is the by-product of unreacted biomass. The vapor and solid phases leave the riser's top and are separated in a cyclone. Sand and char are dropped into a second fluidized bed called a char combustor, where the unreacted char is burned in the air to rewarm the sand. Thus, the biomass itself undergoes partial combustion to generate the energy needed to power the endothermic pyrolysis reactions.

The aqueous and organic phases of the bio-oil can occasionally split from one another. Fast pyrolysis bio-oils have an oxygen content as high as 50% by mass, however, it is commonly accepted that they will undergo hydrotreatment to lower the oxygen level. The simulation model requires the relative amounts of the various oxygenate classes present in the bio-oil which is also an alternative way to describe the dry organics. An RYield reactor block is used to model the major conversion of the fast pyrolysis process. The RYield reactor converts the non-conventional component specified as WOOD into a selected number of model compounds to depict bio-oil. Thereafter the mass yield is calculated externally and routed to ASPEN Plus in an Excel spreadsheet. The light gases and organics inputted in the simulation are selected from ASPEN Plus library components.

Table 3 shows the final analysis of the normalized biomass feedstock, the compositions of the organics and the total pyrolysis yields. A selection of model components used to mix fictitious bio-oil were derived from Heo *et al.*[17] and van Schalkwyk *et al.*[18] to express the organics as library components for the flowsheet simulation. An Excel solver routine uses the normalized biomass feedstocks and bio-oil composition targets from the oxygenate, the ultimate and the product class yields

Table 2 Different model blocks in ASPEN Plus specified in the present model

ASPEN plus ID	Block ID	Description
Riser block	RISER	The riser block is made up of the hierarchy. In the riser, the separator block permits only the biomass feedstock to flow into the RYield reactor named DECON while every other component is not allowed to enter the reactor
Setup calculator	SETUP	This is the main calculator block that is used to set the overall simulation, the constituents of the biomass feedstock, and some operating conditions
Carbon calculator	CARBON CALCULATOR	The amount of carbon used up and produced is accounted for in this block
Sand calculator	SAND2BM CALCULATOR	The required sand needed to heat up the biomass is computed in the sand calculator block
Utility calculator	UTILS CALCULATOR	This specifies the heat duty of the process with respect to work, power
Charcomb combustor	CHARCOMB	In the main flowsheet, the CHARCOMB block makes up the hierarchy. This calculator uses the ultimate analysis of the CHAR to set the flow of oxygen in the split stream and the combustion products yields
Recycle compressor	REC	The noncondensable gases in the gas stream are recycled here
Quench loop	ABSORBER	In the absorber, impurities in the gas–liquid stream, are removed to enhance the efficiency of the flow process

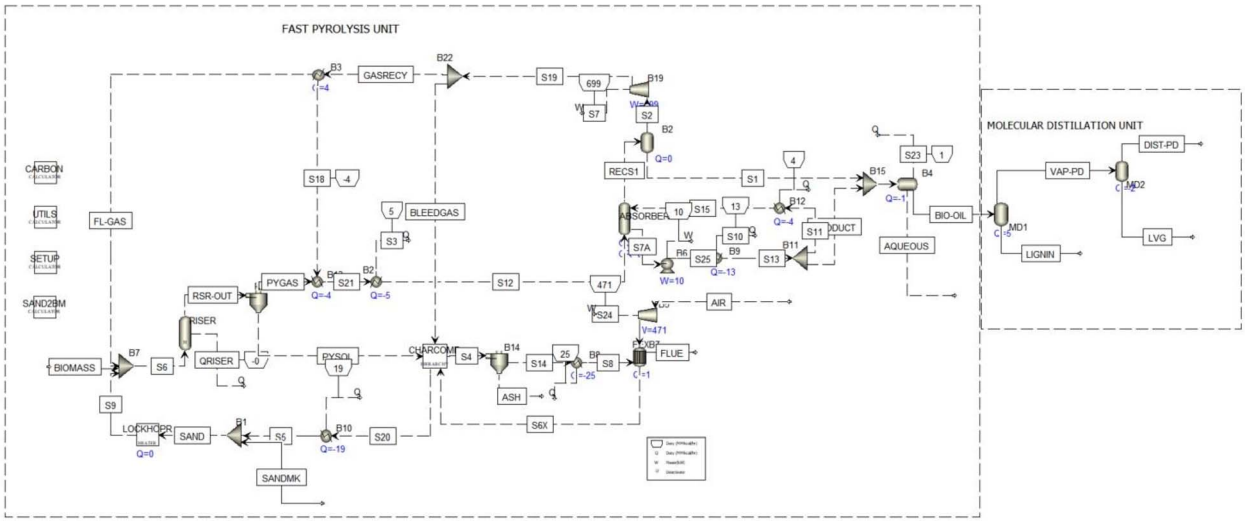

Fig. 1 Overview of the flowsheet for the integration of molecular distillation with fast pyrolysis of biomass.

Table 3 Normalized biomass feedstock and bio-oil compositions

Rice husk				Forestry residues			
Product class (dry wood basis)		Organics composition oxygenate class (sum to 69.3%)		Product class (dry wood basis)		Organics composition oxygenate class (sum to 69.3%)	
Gas	7.8%	Acids	1.43%	Gas	15.0%	Acids	2.77%
Organics	69.3%	Phenols	6.08%	Organics	56.3%	Phenols	1.15%
Water	13.7%	Methoxyphenols	26.0%	Water	15.9%	Methoxyphenols	43.3%
Char	9.20%	Levoglucosan	19.2%	Char	12.8%	Levoglucosan	1.91%
		Other oxygenates	16.6%		15.0%	Other oxygenates	7.15%

described in Table 3. The yields gotten from the solver routine is then inputted as the values for the chosen model components in ASPEN Plus. The mixed conventional inert solid, nonconventional (MIXED/CISOLID/NC) was used as the simulation stream class. The biomass and char produced after the pyrolysis process are nonconventional components. However, only the char components are MIXED while the CISOLID components are sand and ash. The ash is due to char combustion. The property package applied in carrying out the simulation is Peng Robinson Bouzard Mathais (PR-BM). This is an ideal choice, especially since the simulation was integrated with molecular distillation for the separation of valuable chemicals or varying oxygen content in the organic phase. PR-BM accurately represents the non-ideal behaviour and self-association of polar, hydrogen-bonding chemicals, which can be separated when integrated with molecular distillation. The operation of the absorber and oil–water separator with PR-BM may not be optimal given the content of the organic materials, which are strongly oxygenated. Alternatively, only these operations could be modelled using Non-Random Two-Liquid (NRTL) or UNIF-DMD property method.

The size of the simulation, the component of the incoming biomass, and a few other variables were configured using the top-level calculator block SETUP. The flowsheet is scaled to a dry wood feedstock rate of 50 000 kg h^{-1}. This is less than half of the 2000 MT d^{-1} standard for commercial biorefineries set by NREL. The feed is divided between two identical riser and combustor sections as observed in the process design of Dutta *et al.*[19] There is 10% moisture entering the feed. The final analysis specifies the biomass content. The calculator block automatically resolves the proximate and sulphur analysis after normalizing the input. The calculator block is then used to set further high-level design parameters. The pyrolysis temperature ought to match the product slate that was previously solved. The dry mass basis for sand to biomass ratio was chosen as 7, which is typical. A Design-Spec will set the temperature of the circulating sand in the simulation. The circulating temperature must not change, and the flow ratio must. The ratio of the sand flow rate to the fluidizing gas flow determines the flow rate. Lift in the riser is ultimately a function of mass flow even though the gas mix and MW are variable, hence the ratio is on a mass basis. The lowest gas flow, where the solid's velocity is equal to its predicted terminal velocity, is what ensures fluidization (in the opposite direction). Since this model cannot resolve these specifics, a conservative ratio of 10% is utilized.

The hierarchy depicted in the riser hierarchy is contained in the RISER block on the main flowsheet. Only the biomass component is sent *via* the Sep block to the RYield reactor

DECON; all other components are sent elsewhere. The mass yields from Excel are put into DECON together with NC characteristics for CHAR. The pyrolysis temperature is given in PYTEMP by the SETUP calculator. The other blocks' temperature requirements are irrelevant; instead, the sand temperature will be changed to ensure adiabatic operation, which implies that the hierarchy (PYQ) has a total duty of zero. Following Fig. 1, the combustor takes in both the unrecycled fraction of the non-condensible gases, which are MIXED components, and the NC solids that are expelled from the pyrolysis riser. It is simple to represent the combustion of MIXED components with RSTOIC, while the combustion of NC CHAR requires RYIELD. The hierarchy depicted in Fig. 1 is contained in the CHARCOMB block on the main flowsheet. In this hierarchy, user interaction is not necessary. Based on the final CHAR analysis, a calculator determines the slipstream oxygen flow and the yields of combustion products. Through the second Sep block, the ash component of CHAR is transformed into the CISOLID component ASH, which is released with the combustion gases. A Design-Spec establishes the airflow for a 2% mole percentage of oxygen in the exhaust, and all blocks are specified as adiabatic.

2.3 Molecular distillation simulation setup

The choice of viable chemicals for isolation and separation was vital for establishing the importance of this research work. Two sets of variables were employed; the molecular weight and boiling point of the compounds as well as the quantity separated and the market price of the compound respectively. Lignin, 1,2-benzenediol, levoglucosan 4-vinyphenol, mnapthen, *p*-hydroquinone, and methyl-salicylate were isolated due to their economic value as well as their quantities present. Also, they were selected due to the significant difference in their boiling point and molecular weight. Phenol compounds such as 4-vinyphenol is an important bio-based platform chemicals that are used in producing reagents for manufacturing plastics, the cosmetics industry, household products.[20] Also, a previous study by Omoriyekomwan *et al.*[21] achieved the enrichment of phenol compounds through the catalytic microwave pyrolysis of palm kernel. Pyrolytic lignin can be used in the production of high-quality liquid fuels.

In this work, ASPEN Plus® V12 was used to imitate a real-life scenario of separating valuables from rice husk pyrolyzed bio-oil. Hence, the thermodynamic properties of the bio-oils must be accurately represented and so, the choice of an appropriate thermodynamic model becomes very crucial. The selection of the thermodynamic model to determine the liquid activity coefficient and equation of state (EOS) is important in the prediction of phase equilibrium. The former covers for differences from ideality in a mixture while the latter explores the relationship between state variables, such as temperature, pressure, and volume, to estimate states of gases. The thermodynamic model selected was based on the comprehensive phase equilibrium modeling analogies by Walas.[22] For the liquid coefficient method, Non-Random Two-Liquid (NRTL) and Universal Quasi-Chemical (UNIQUAC) were examined. These activity coefficient methods can handle any group of non-polar and polar compounds. Most importantly, they can strongly describe the liquid–liquid equilibrium and non-ideal mixtures of a system. Thus, these features are valuable since bio-oil is a complex mixture that undergoes phase separation. The phase equilibrium of the system is measured using binary parameters based on the linear regression and experimental data obtained from literature which is deposited in Aspen Physical Property Databanks. Therefore, the NRTL model was chosen using the technique by Waals since the model achieves the best fit experimental data when illustrating an organic mixture.

The Redlich–Kwong and Hayden O'Connell equation of state method was examined. However, the Hayden O'Connell equation of state with exceptional in the analysis of dimerization effects, robust association, and solvation effects couldn't be used as HOCETA binary parameters in literature and Aspen property bank was unavailable. Accordingly, Redlich–Kwong model which is sufficient for non-ideal vapor phase and components with low to medium pressures was used. This model depends on the use of empirical derived constants; measurement of attraction between molecules and co-volume (a), (b) respectively to predict properties of components, critical temperature (T_c), and critical pressure (P_c) as shown by eqn (2.1)–(2.5).

$$P = \frac{RT}{V_{m-b}} - \frac{a}{\sqrt{T}\,V_m(V_m + b)} \tag{2.1}$$

$$a = \sum_i x_i a_i \tag{2.2}$$

$$a_i = \frac{0.42748 R^2 {T_{c,i}}^2}{P_{c,i}} \tag{2.3}$$

$$b = \sum_i x_i b_i \tag{2.4}$$

$$b_i = \frac{0.08864 R T_{c,i}}{P_{c,i}} \tag{2.5}$$

The co-volumes represent four times the volumes occupied by the total number of molecules as specified by van der Waal's application of hard spheres. Therefore, the physical space between molecules cannot be shared which implies that the minimum displacement between the two molecules center is double the radius of the sphere. Otherwise, the particles would enter spheres of one another annulling the hard sphere model and the effective molecular diameter of a single component can then be calculated by eqn (2.6). However, the mean free paths can only be determined when the temperature and pressure of optimal separation are combined.

$$d = \left(\frac{6V_p}{\pi}\right)^{\frac{1}{3}} \tag{2.6}$$

Thereafter, the effective molecular diameter d, is then substituted into the mean free path eqn (2.7). The mean free path of an ideal molecule, as shown by eqn (2.7),[23] provides the

displacement where there is a certain prospect of no molecular collisions. The symbols d, N_A, R, P and T represent the effective diameter of the molecule, Avogadro's number, ideal gas constant and the system temperature and pressure in SI units respectively. The mean free path, λ as shown in eqn (2.7), is inversely proportional to the effective diameter of a molecule squared. This implies that larger molecules have smaller mean free paths and *vice versa*.

$$\lambda = \frac{RT}{\sqrt{2}\pi d^2 N_A P} \quad (2.7)$$

The focus of the simulation of the molecular distillation process is to comparatively predict and favor the isolation and recovery of valuable chemicals and fuels such as levoglucosan, 4-vinyphenol, *p*-hydroquinone, and pyrolytic lignin. The first task of the simulation was to evaluate the influence of temperature on the vapour pressure of the components to understand the extent of separation through the volatility tendency shown by the compounds. This was computed by the ASPEN pure component analysis with a fixed pressure of 1 Pa and temperatures between 30 and 100 °C. Flash vessels were selected to represent the Molecular distillation (MD) process because ASPEN Plus does not have a molecular distillation operation tool in its database. Two-phase flash vessels were used for the separation model denoted as MD1 and MD2. The MD1 simulation is for the separation of the pyrolytic lignin (enhancing the recovery and purity of the pyrolytic lignin as well as ensuring the recovery of the key chemicals) while the MD2 simulation solely accounts for the recovery and purity of furfural, acetic acid, and phenol.

The product stream (DIST-PD) and product stream (LVG) represent the distillate and the levoglucosan stream respectively. The biomass feed rate of 0.4 kg h^{-1} for the rice husk and forestry residues was chosen for this simulation since the configuration of most molecular distillation equipment for research analysis has a feed rate between 0.1 and 0.4 kg h^{-1} which can attain vacuum pressures of 0.1 Pa.[24]

The number of iterations was kept at 30 maxima with an error tolerance of ±0.0001 to annul unnecessary long-run iteration times, and standard convergence parameters were maintained. However, after the evaluation of MD separation, sensitivity analysis was performed in ASPEN Plus ® to further understand the behavior of component separation under different operating conditions. Table 4 shows the operating conditions for the separation of pyrolytic lignin, levoglucosan, 1,2-benzenediol, 4-vinyphenol, mnapthen, *p*-hydroquinone, and methyl-salicylate for MD1 and MD2 simulations.

Table 4 Operating conditions for MD1 and MD2 simulations

Simulation	Operating conditions
MD1	Bio-oil feed at 25 °C and 1 Pa System pressures: 0.1–30 Pa Evaporation temperatures: 50–130 °C; 10 °C intervals
MD2	System pressures: 0.1–30 Pa Evaporation temperatures: 40–80 °C; 10 °C intervals

Wang *et al.*[16] carried out experimental research with the KDL-5 molecular distillation apparatus using the bio-oil produced from the pyrolysis of Mongolian pine sawdust for a single separation process. He observed that the volatile components evaporated from the feedstock in the temperature range of 30–130 °C, hence a temperature of 30 °C was chosen as the minimum temperature for this simulation. The starting temperature for MD2 simulations was reduced to accommodate the dense viscous compounds which eventually separated into the product stream containing the residue. The liquid mass flow rates for each compound were recorded to ascertain the purified quantity of liquid levoglucosan, 1,2-benzenediol, 4-vinyphenol, mnapthen, *p*-hydroquinone, and methyl-salicylate, for efficient chemical separation.

3 Results and discussions

3.1 Model validation

To validate the fast pyrolysis model, the yields of the pyrolysis products and the ultimate composition of rice husk and forestry residues bio-oil from the simulation were compared against experimental data. The comparison between the simulation and experimental results is illustrated in Table 5.

In Table 5, the findings observed implies that there is a high degree of agreement between the results obtained from the simulation and that of the experiment. There is a minimal variation between the simulation and experimental with respect to the product yields of the pyrolysis process which is less than 13%. It is worth noting that the yields of the bio-oil and biochar were predicted slightly higher by the developed model of this work. For the carbon content of the bio-oil, it can be seen from Table 4 that there is no variation between the experimental and simulation results for both the rice husk and forest residues. While for the hydrogen, sulphur, oxygen and nitrogen, the discrepancy could be due to impurities and dust particles which was not accounted for when developing the model. This is similar to the predictions observed in the study carried out by Hasan *et al.*[25] Nonetheless the agreement between the simulation and experimental results is still reasonably high.

To ascertain the carbon tracking and utility usage, for the 50 000 kg h^{-1} rice husk and forestry residues biomass described above, their carbon balances are given in Table 5, with a conversion of approximately 71% for both rice and forestry residues.

In Fig. 2, the carbon balance shows the amount of bio-oil achieved in the fast pyrolysis of the selected biomass feedstocks. Also, the aqueous loss and the flue gas loss are accounted for as shown above.

3.2 The effects of pyrolysis conditions

Pyrolysis temperature is an important parameter that affects the products. The pyrolysis products were produced at the reaction temperatures ranging between (350 °C and 550 °C). Fig. 3 illustrate the yields of the fast pyrolysis gas and bio-oil yields at varying temperatures. It can be seen from Fig. 3(left) that in both the rice husk and the forestry residue biomass feedstocks

Table 5 The fast pyrolysis products yields, and the bio-oil composition obtained from the simulation and experiments

	Yield (wt%)			Yield (wt%)	
Pyrolysis products	Simulation	Experiment	Composition of bio-oil	Simulation	Experiment
Rice husk					
Bio-oil	71.0	60.0	Carbon	53.5	53.5
Biochar	26.7	25.2	Hydrogen	4.31	7.0
Syngas	2.12	14.8	Nitrogen	0.03	1.4
Forestry residues					
Bio-oil	47.1	45.2	Carbon	48.0	48.0
Biochar	31.6	28.8	Hydrogen	6.50	6.36
Syngas	21.3	26.1	Nitrogen	0.7	0.12
			Sulphur		0.06

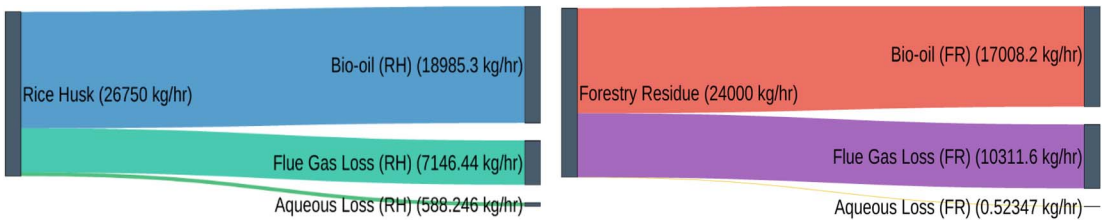

Fig. 2 The carbon balance for the fast pyrolysis of rice husk (RH) and forestry residues (FR) biomass feedstock.

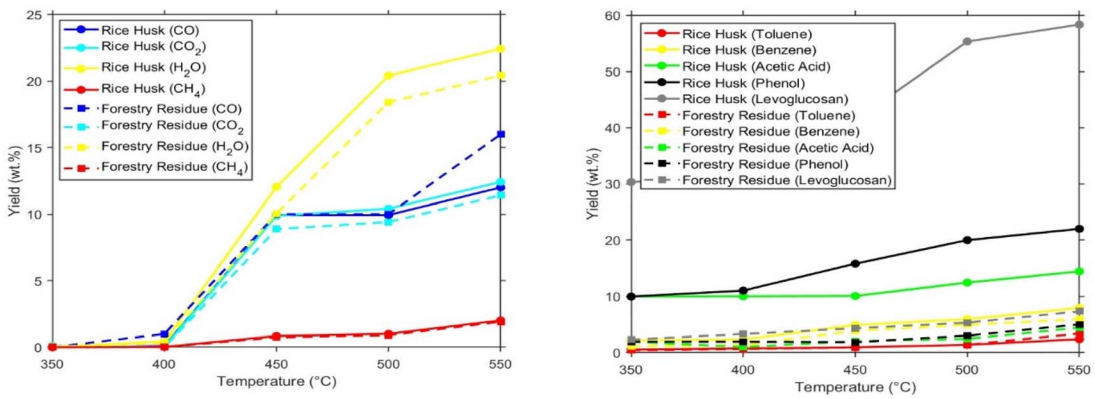

Fig. 3 Resulting yields of the fast pyrolysis for (left) gas and (right) bio-oil at varying temperatures.

the gas yields for CO, CO_2, H_2O, and CH_4 increased gradually with increasing temperatures. Similarly, in Fig. 3(right), it is observed that the yields of the major bio-oil compounds present in both biomasses increased with an increase in the temperature. The findings from the experimental analysis of rice husk of Heo *et al.*[17] showed that the gas yields increased with increasing pyrolysis temperatures which agrees with the results from this work. The increase in gas yield can be attributed to the secondary cracking of the fast pyrolysis of char and vapors into the gas.

3.3 The effects of the biomass types

The comparison of the overall yields of the pyrolysis products present in the rice husk and the forestry residue model is shown in Fig. 4. It can be observed that the highest yield of the pyrolysis compound was levoglucosan for rice husk and mnapthen for forestry residues respectively.

From Fig. 4, it can be observed that the pyrolysis of the rice husk model from the simulation of this work produced a high amount of phenol including 4-ethylphenol, 3-ethylphenol, pheno-01, 1,2-benzenediol, 4-vinylphneol, 2,4-dimethyl and isoeugen which makes up 50.4% while alcoholic yields such as levoglucosan and other components provided 49.6%. This outcome was compared with the study by Li *et al.*,[26] on the experimental analysis of rice husk pyrolysis it was detected that after pre-treatment of the rice husk, the yield of components produced was 18.7% acids, 22.5% ketones, 16.9% esters, and 17.9% of phenols. This variation in yield can be attributed to

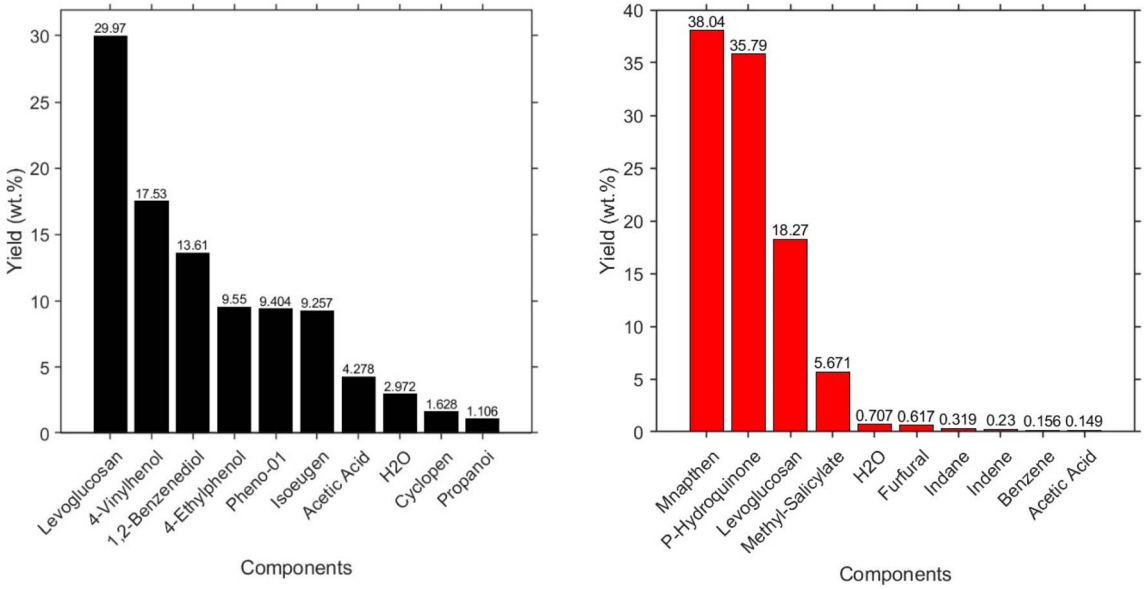

Fig. 4 Comparison between the overall pyrolysis yields for (left) rice husk and (right) forestry residue biomass.

factors such as; the pre-treatment type used for the rice husk, the temperature and pressure of the pyrolyzer, and the type of pyrolysis (fast or slow) used for the experimental work.

Similarly, the same analysis was performed for the forestry residue model. It can be seen that the pyrolysis of forestry residue simulated in this work, resulted in a high yield of 73.7% aldehydes which includes methyl-salicylate and furfural. However, there was a low yield of alcohol components such as levoglucosan which was made up of 5.90% while the remaining components provided 20.4%. This result was compared with the experimental findings obtained by Paul *et al.*[27] from which it was observed that after pre-treatment of the forestry residue, 27.8% of aldehydes, 3.0% of levoglucosan, and 12.3% of acid were produced. Thus it was noted that both in the experimental and simulated analysis of the pyrolysis of forestry residue, levoglucosan yield will not be favoured. Therefore, this further affirms that the rice husk is a better feedstock for pyrolysis when levoglucosan is been considered as the target component of interest.

Additionally, the yield of levoglucosan which is a major component of both the rice husk model and the forestry residue model achieved from this work was compared to that of the experiment as shown in Table 6. Moreover, previous studies carried out by Wang *et al.*,[24] and Guo *et al.*[28] revealed that levoglucosan with a boiling point of about 380 °C becomes isolated from molecules of lower molecular weight when the operating conditions of the molecular distillation unit were maintained at 60 Pa and 100 °C. The separation was observed to have occurred without coking and contamination of anhydrosugars, which are typical limitations of other distillation systems. Wang *et al.*[24] also carried out an experiment using red oak biomass and observed a 75% recovery of levoglucosan from the final output. Whereas this work has given a percentage recovery of 98.72% and 97.41% for rice husk and forestry residue as shown from the optimized simulated results in Section 3.4.2 MD2.

3.4 Molecular distillation results

To optimize the molecular distillation unit, sensitivity analysis was performed to observe the effect of incremental changes in the process conditions for rice husk and forestry residue biomasses. The bio-oil compounds were selected due to their uses in the chemical, petrochemical, paint, clothing, and textiles industries. For instance, 4-vinylphenol is an important bio-based platform chemical that is used in producing reagents for manufacturing plastics, the cosmetics industry, and household products.[26] The range of values simulated for the temperature and pressure of the system was 10–90 °C and 0.1–30 Pa respectively. The major valuable chemicals observed for rice husk include levoglucosan (LVG), 4-vinylphenol (4-VINYLP), and 1,2-benzenediol. While for forestry residues mnapthen ($C_{11}H_{10}$-1), *p*-hydroquinone ($C_6H_6O_2$), methyl-salicylate ($C_8H_8O_3$), and levoglucosan (LVG). These compounds were simulated to ascertain the sensitivity of both models. The molecular distillation unit was simulated, with the lignin component recovered first from the process in the MD1 flash vessel before entering into the MD2 flash vessel where key compounds of interest were separated and purified. It is worth noting that, in this study, levoglucosan was not only recovered but also purified.

3.4.1 MD1. In this study, it was noticed that for both the rice husk and the forestry residue biomass, there was no output flow of lignin material in the pyrolytic lignin stream of the MD1 flash vessel. This validates the theory of Mei *et al.*[37] which suggests that for the primary reaction of lignin, with increasing temperature, the production of phenolic monomers is enhanced significantly due to the increasing conversion rate of lignin. However, due to the secondary reaction occurring with the extension of reaction time, more phenolic monomers would be transformed into light gases. Also, according to Hang Seok Choi,[38] fast pyrolysis involves heating the reactor's contents

Table 6 Comparison of the pyrolysis yield (wt%) of this work with previous studies

S/n	Biomass feedstock	Method of study	Pyrolysis process conditions	Bio-oil yield (wt%)	Reference
1	Douglas-fir wood	Simulation (kinetic modeling)	Simulated fast pyrolysis at 500 °C; residence time 1–2 s; fluidized bed reactor conditions	68% (carboxylic acids (*e.g.*, acetic acid): 10–20%; phenolic compounds: 5–10%, 15–25% levoglucosan	Bu *et al.*[29]
2	Pure cellulose	Experimental	Fast pyrolysis at 400–600 °C, heating rate 10^3–10^4 K s^{-1}, vapor residence time < 2 s	75% of levoglucosan with minor amounts of other anhydrosugars	Hakeem *et al.*[30]
3	Eucalyptus	Experimental	Fast pyrolysis with H_2SO_4 impregnation (0.25–1.25 wt%)	3.6–21.3% (levoglucosan yield)	Zhang *et al.*[31]
4	Corncobs	Experimental	Fast pyrolysis with H_2SO_4 impregnation (up to 2.75 wt%)	38.5% levoglucosan yield) selective production of anhydrosugars with furfural as a co-product	Fan *et al.*[32]
5	Microcrystalline cellulose	Experimental	Microwave-assisted pyrolysis (200–300 °C, 150–300 W)	2–9% (levoglucosan yield)	Nieva *et al.*[33]
6	Cotton straw	Experimental	Fluidized bed reactor at 500 °C, 1.4 s holding time, 8% acid concentration	13.2–19.3% levoglucosan yield	Wang *et al.*[34]
7	Sugarcane bagasse	Experimental	Micropyrolysis at 350–600 °C	Highest levoglucosan yield of 39 wt% at 400 °C	David *et al.*[35]
8	Red oak	Experimental	Staged-collection system, pyrolysis at 450 °C	87% anhydrosugars with levoglucosan 29.4 wt% as a major component	Rover *et al.*[36]
9	Rice husk and forestry residue	Simulation	Fluidized bed reactor at (350–550 °C), 0.1 Pa to 30 Pa	29–60% levoglucosan yield and 40% made up of other compounds such as acetic acid, phenol, furfural	This work

rapidly to the desired temperature (often between 450 °C and 600 °C), breaking down lignin into volatiles that swiftly condense into liquid. The conversion of lignin is more efficient and practical due to the quick pyrolysis process's adaptability and simplicity. In this study, the fast pyrolysis occurred at temperatures between 350 °C and 550 °C, and thus suitable to deduce that this process led to the decomposition of all lignin composition in the biomass. Hence no lignin was recovered as a by-product for rice husk and forestry residue biomass respectively.

3.4.2 MD2. The MD2 flash vessel was used to separate levoglucosan amongst other chemicals. The fast pyrolysis of the rice husk and forestry residue biomass produced several compounds that are constituents of bio-oil. Thus, in this study, our major interest was in the separation of valuable chemicals such as levoglucosan, 1,2-benzenediol, and 4-vinylphenol. However, upon recovery of the levoglucosan, it was also purified due to the high quantity present in the MD2 stream. Moreover, high-value renewable chiral building blocks like levoglucosan can be utilized to produce a variety of bio-based fine chemicals, polymers, and green solvents.[39]

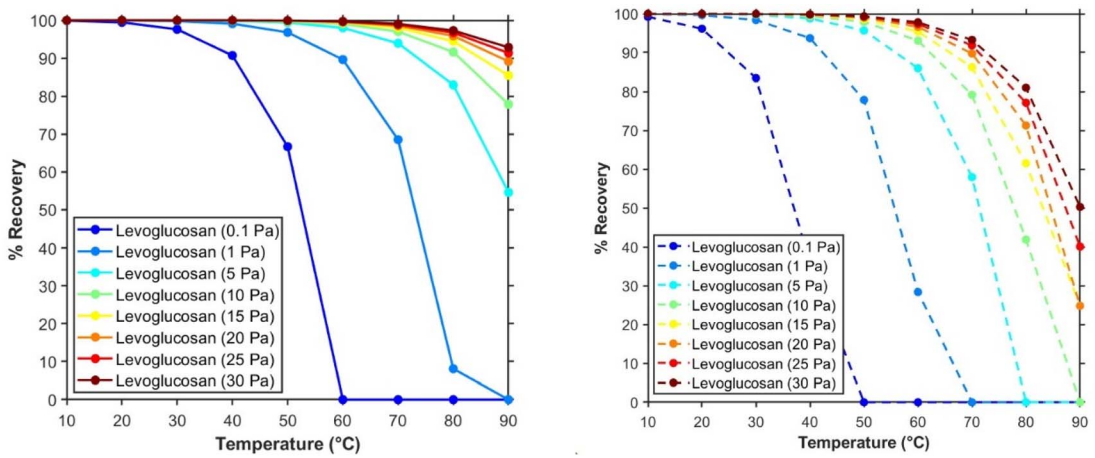

Fig. 5 The % recovery of levoglucosan at varying temperatures and pressures for (left) rice husk and (right) forestry residue models.

From Fig. 5 (the numerical data for Fig. 5–10 can be found in the ESI†), it can be deduced that the theory of mean free path greatly affects the recovery of levoglucosan. Thus it can be seen that the highest recovery occurred at lower temperatures and lower pressures. This implies that the mean free path of levoglucosan is maximized, which allows more molecules to get to the evaporator to be condensed enhancing recovery. However, there was a huge variation in the percentage recovery of the rice husk and forestry residue models. The rice husk model had its highest recovery at an operating condition of 1 Pa and 10 °C while all other pressures above 1 Pa, yielded the same percentage recovery. The levoglucosan feed recovered was 99.98%. Moreover, for the forestry residue model (see ESI†), the optimal pressure for the MD2 was 30 Pa, and above this pressure yielded the same percentage recovery. The temperature for the highest recovery of levoglucosan was detected to be 10 °C and the amount of levoglucosan recovered at this operating condition was 99.96%.

Therefore it can be inferred that the rice husk model had a higher percentage of levoglucosan recovered than the forestry residue model. Nevertheless, to ascertain this possibility, other important parameters such as the amount and purity of levoglucosan produced would have to be considered. It is worth noting that the separation of levoglucosan is highly dependent on the theory of the mean free path of a molecule. The mean free path of a molecule is the average distance that a molecule can move in between collisions and is dependent on some process parameters such as the pressure, temperature, diameter, and size of the molecule.[40] Moreover, in Fig. 5 for both models, it can be seen that as the pressure increased, there was a corresponding increase in the recovery of levoglucosan. This implies that more amount of levoglucosan would be obtained from the MD2 unit with higher operating pressure. Thus, this validates the theory of mean free path where increased pressure hinders the distance traveled by molecules without collision with another molecule.[41] Therefore, the higher the pressure of a vessel, the more collisions the molecules will tend to experience, thus leading to a reduced number of molecules getting to the condenser and hence a decrease in the evaporation rate.

Furthermore, it can be seen from Fig. 5 to Fig. 7 that an increase in the operating temperature of the MD2 unit led to a reduction in the amount of molecules recovered. Andrea *et al.*[42] in their study for the simulation of the molecular distillation process for lactic acid it was shown as the temperature increases, the mean free path of evaporated molecules increases, thereby extending the possible distance of travel without molecular collisions. As such, in line with this study, the number of molecules reaching the condenser surface increased. Hence, this explains why the concentration of components in the residue decreases with temperature. Accordingly, when reduced molecules are available in the residue stream *i.e.* the LVG stream of the MD2, there would be lower recovery of levoglucosan and other components which is observed to be the case for both models in this study. It is worth noting that, despite the high amount of recovery of levoglucosan due to an increase in pressure as observed in Fig. 5, it also comes with a reduced level of purity in the LVG stream of MD2. This can be seen in Fig. 6 below.

In Fig. 7, a comparison of both figures showed that as the pressure was increased, the percentage purity of the recovered levoglucosan was reduced at a higher pressure when the temperature was kept constant. This indicates that, at an operating temperature of 10 °C, the percentage purity of levoglucosan at 0.1 Pa is 99.73%. However, at a pressure of 30 Pa, the recovery of levoglucosan was observed to be about 52.34% which shows that a purer amount of levoglucosan was recovered at a lower pressure in the rice husk model. Similarly, for the forestry residue model, it was noticed that at 10 °C and 0.1 Pa, levoglucosan's purity was 98.41%. Whereas at 30 Pa, it was 49.82% which is a lower value than the former, thus both models are deduced to follow the same pattern as regards pressure variation and purity percentage.

Furthermore, the analysis below shows that with an increase in the operating temperature of the MD2 unit, the percentage

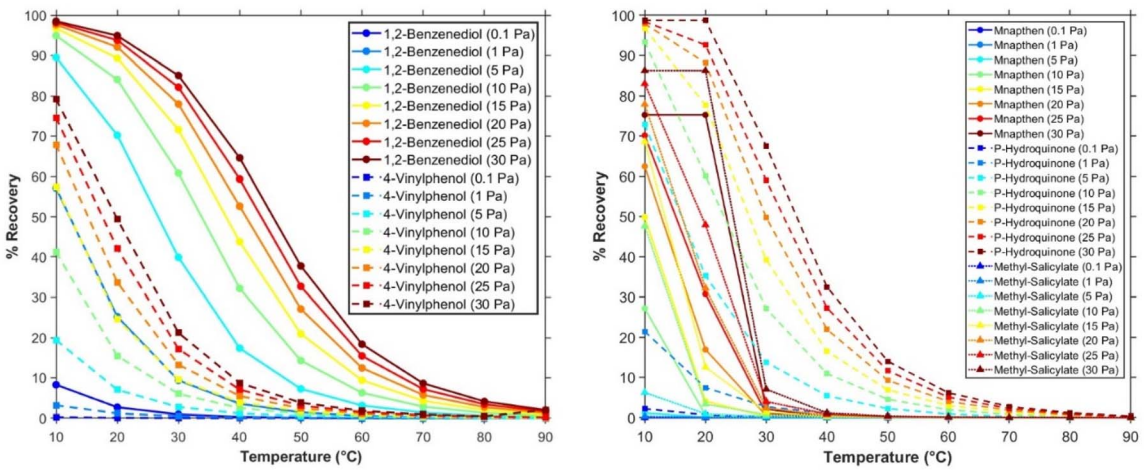

Fig. 6 (left) The % recovery of rice husk (levoglucosan, 1,2-benzenediol, and 4-vinylphenol) and (right) forestry residue (mnapthen, *p*-hydroquinone, and methyl-salicylate) models isolated compounds at varying temperatures and pressures.

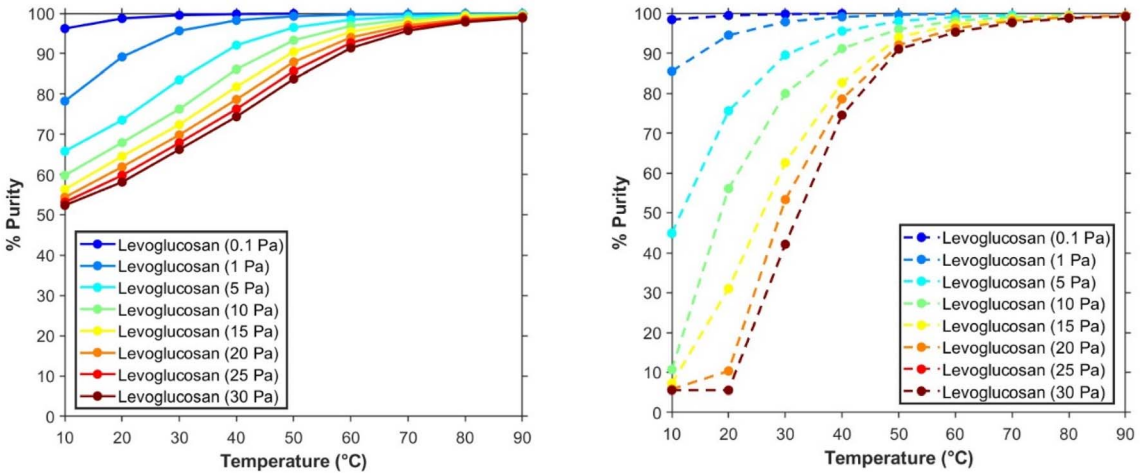

Fig. 7 The % Purity of levoglucosan in the LVG stream of MD2 at varying temperatures and pressure for (left) rice husk and (right) forestry residue model.

purity also increased. It could be observed that the highest purity about 99.89%, was obtained at 50 °C and 0.1 Pa for the rice husk model whereas 99.10% purity at 40 °C and 0.1 Pa for the forestry residue model. Consequently, this implies that temperature would vary proportionately with the percentage purity of the levoglucosan recovered. This validates the theory that the mean free path of molecules will vary proportionately with temperature and inversely with pressure,[39] since at higher temperatures, there will be a reduced amount of molecules in the residue stream, from the literature, considering the rice husk model, it was observed that levoglucosan had a boiling point of about 384 °C, and the major impurities which are 4-vinylphenol has a boiling point of about 228.5 °C and 1,2-benzenediol a boiling point of 245 °C, as the temperature increases, more molecules of both 1,2-benzenediol and 4-vinylphenol moved to the condenser and thus evaporated faster than the corresponding molecules of levoglucosan.

Additionally, for that of the forestry residue model, the boiling points of the major impurities noticed were mnapthen, *p*-hydroquinone, and methyl-salicylate with their boiling points as 220 °C, 277 °C, and 285 °C respectively while the levoglucosan has a boiling point of 384 °C. Thus as the temperature does increase, the molecules of impurities will easily gain a higher mean free path than the molecules of levoglucosan, thus the purity of levoglucosan recovered was bound to increase, while the amount recovered would decrease. The major importance of the MD2 unit was to maximize the purity of levoglucosan while maintaining a high percentage recovery. The major impurities observed in the LVG stream of the rice husk model and that of the forest residue model in the MD2 unit were 1,2-benzenediol and 4-vinylphenol (for model I) and mnapthen, *p*-hydroquinone, and methyl-salicylate (for model II) respectively. The analysis of the mass flow rate of these impurities as well as levoglucosan was carried out and is tabulated in the ESI.† A

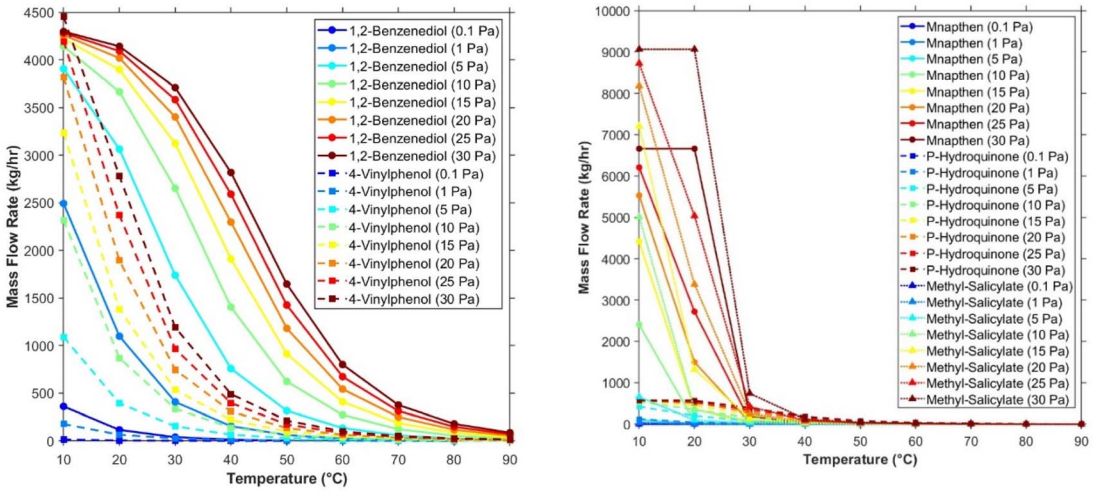

Fig. 8 The mass flow rate of isolated compounds at varying temperatures and pressures in the LVG stream of MD2 unit for (left) rice husk and (right) forestry residue models.

graphical representation of this data was made for easy analysis of the result obtained which is illustrated in Fig. 8.

From Fig. 8, it can be noticed that there was a greater amount of 1,2-benzenediol as an impurity than 4-vinylphenol in the rice husk model. Thus, this can be attributed to the boiling point of the molecules of 1,2-benzenediol and 4-vinylphenol which are 245 °C and 228.5 °C respectively. Moreover, from Fig. 7(right), it was observed that methyl-salicylate contributed the highest amount of impurity, closely followed by *p*-hydroquinone and the least mnapthen. This could also be due to the difference in their boiling point, as a value of 285 °C, 277 °C, and 220 °C respectively is obtained from literature as the boiling point of these impurities. Therefore, this implies that more molecules of lower boiling point will easily be evaporated than molecules of higher boiling point. It can also be deduced that the mass flow rate of both impurities would increase as the operating temperature reduces and *vice versa*. This depicts that more of their molecules would have a greater mean free path as their temperature increases.

Hence, this occurrence suggests that an elevated temperature should be chosen for the simulation of this study to minimize the amount of impurities from other compounds.

Also, from Fig. 9, it can be seen that the mass flow of levoglucosan reduced with an increase in the operating temperature of the unit. However, there was a decrease in mass flow rate when the operating pressure was reduced. It can also be deduced from Tables C and D (see ESI)† that the amount of levoglucosan produced from the rice husk model is greater than the amount from forestry residue. This is in agreement with Hakeem *et al.*[30] study, which postulated from their experimental analysis that the formation of levoglucosan from biomass pyrolysis amongst other biofuels is dependent on several factors. Some of these factors include the physicochemical properties of biomass, such as particle size, crystallinity, and degree of polymerization (DP) which were observed to have a significant influence on the yield of levoglucosan during pyrolysis. On further review carried out by Zhang *et al.*,[43] it was observed that smaller particle sizes generally favor uniform and rapid heating, reducing heat transfer limitations and enhancing the yield of levoglucosan. Larger particle sizes often result in non-uniform heating, leading to higher char formation and lower levoglucosan yield due to slower heat transfer and secondary reactions.

Additionally, Zhang *et al.*[43] investigation showed that rice husk had smaller particle sizes (primarily between 0.45 and 0.9 mm) than forestry residue which consists of larger and more irregular particle sizes. Thus resulting in a larger amount of levoglucosan produced from the rice husk compared to the forestry residue as shown in Tables C and D (see ESI).† In the case of crystallinity, Zheng *et al.*[44] observed from experiments that the crystallinity of cellulose impacts its thermal stability and reactivity during pyrolysis. Highly crystalline cellulose requires higher temperatures for decomposition, while amorphous cellulose degrades more readily at lower temperatures, favoring levoglucosan production. Also, previous work by Wang *et al.*[16] indicates that amorphous cellulose tends to yield higher quantities of levoglucosan at lower pyrolysis temperatures (around 500 °C), while crystalline cellulose produces more levoglucosan at elevated temperatures. The study from Zhang *et al.*[43] reveals that moderate crystallinity in rice husk cellulose promotes a balance between thermal stability and efficient decomposition while forest residues generally have higher crystallinity. This high crystallinity delays cellulose decomposition as more energy is required to break down the organized, dense cellulose structure. Therefore, the operating temperature of the pyrolysis would not be sufficient to provide the energy needed for the formation of levoglucosan, thus affirming the yield from the MD1 unit.

Furthermore, as was observed by Zhang *et al.*[43] The DP of cellulose affects the pyrolysis reaction rate. Lower DP cellulose decomposes more rapidly, producing higher levoglucosan yields. Conversely, higher DP cellulose requires longer heating

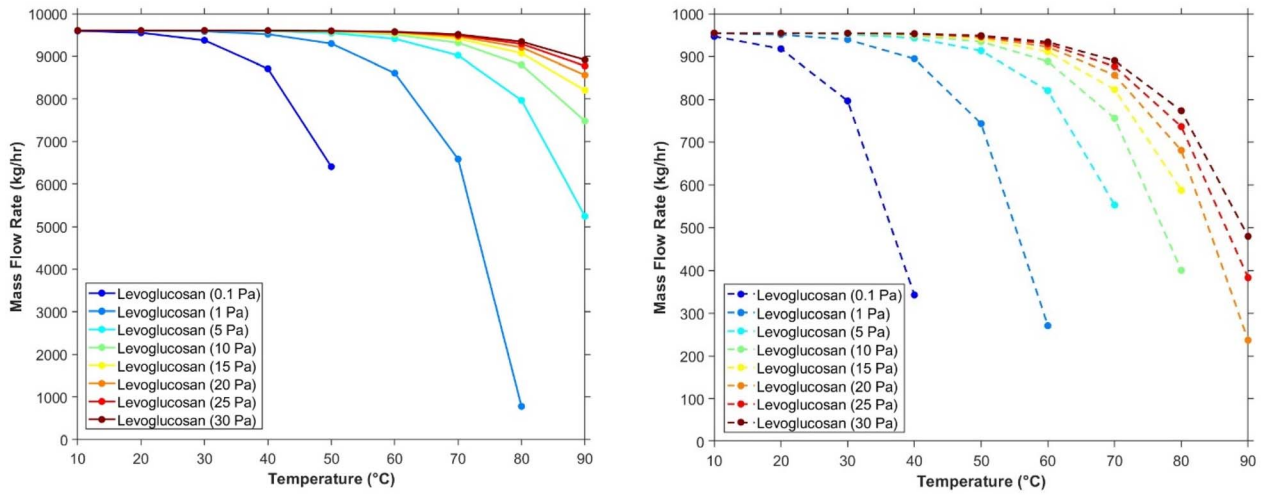

Fig. 9 The mass flow rate of levoglucosan, at varying temperatures and pressure in the LVG stream of MD2 unit for (left) rice husk and (right) forestry residue models.

time, which may increase secondary reactions that reduce levoglucosan yield. Rice husk was observed to have a cellulose with a lower degree of polymerization, meaning the cellulose chains are shorter, unlike forest residue which exhibits a longer degree of polymerization and thus would require more energy to break down the long chain. These physicochemical properties of rice husk and forest residue validate the results from the simulation as shown in Tables C and D (see ESI)† that levoglucosan production will be more favoured in the former than the latter.

Moreover, in this work, the fluidized bed reactor was applied in simulating the fast pyrolysis for the biomasses due to its efficient heat transfer, rapid heating rates, and homogeneous temperature distribution. However, the Li *et al.*[26] study showed that the turbulent flow ensures uniform contact between biomass particles and heat, reducing temperature gradients and preventing char formation. Also, the short vapor residence time offered by this reactor prevents the secondary decomposition of levoglucosan into other compounds like furfural or char. Thus, the smaller particle size and moderate crystallinity of rice husks as observed by Zhang *et al.*[43] make them ideal for fluidized bed reactors. These properties enhance heat transfer efficiency, minimizing thermal lag and maximizing levoglucosan production whereas, the larger particle size and higher crystallinity of forest residues create heat transfer limitations even in fluidized bed reactors. The non-uniform heating of larger particles can result in incomplete pyrolysis, reducing levoglucosan yield. This experimental analysis further validates the high yield of levoglucosan from the rice husk model and the low yield from forestry residue.

Nevertheless, from Tables C and D (see ESI),† there was an increase in the mass flow rate for some of the compounds as the pressure increased. This is so since, at a higher pressure, molecules would have a larger number of collisions within themselves and the containing vessel. Thus, their mean free path would be reduced, thereby reducing the number of molecules that can reach the condenser for evaporation to take place.[41] Considering the necessity to optimize both the percentage recovery and purity of levoglucosan, a sensitivity analysis was carried out. The most optimum operating condition was chosen by multiplying the values of both the recovery and purity percentages as well as choosing the best output after the combination. Fig. 10 show that the optimal operating condition for the rice husk model was 20 °C and 0.1 Pa while that of the forestry residue was 10 °C and 0.1 Pa.

The combined % purity and % recovery of levoglucosan at the chosen operating conditions were 99.45% and 98.72% for the rice husk, 98.21% and 97.41% for the forestry residue biomass. On comparison of both models, it can be deduced that the rice husk model offers a better production of levoglucosan than the forestry residue model, based on the analysis carried out. The rice husk model's optimal operating condition gave a better combined percentage purity and recovery of 98.12% than that of the forestry residue which was 96.43%.

Furthermore, a comparison of the desired product yield was also considered from the biomass feed flowrate simulated for both models which was 100 kg h^{-1}. The resulting mass flow rate of levoglucosan for rice husk was 9551.9 kg h^{-1} at the optimal operating condition is far greater than that of the forestry

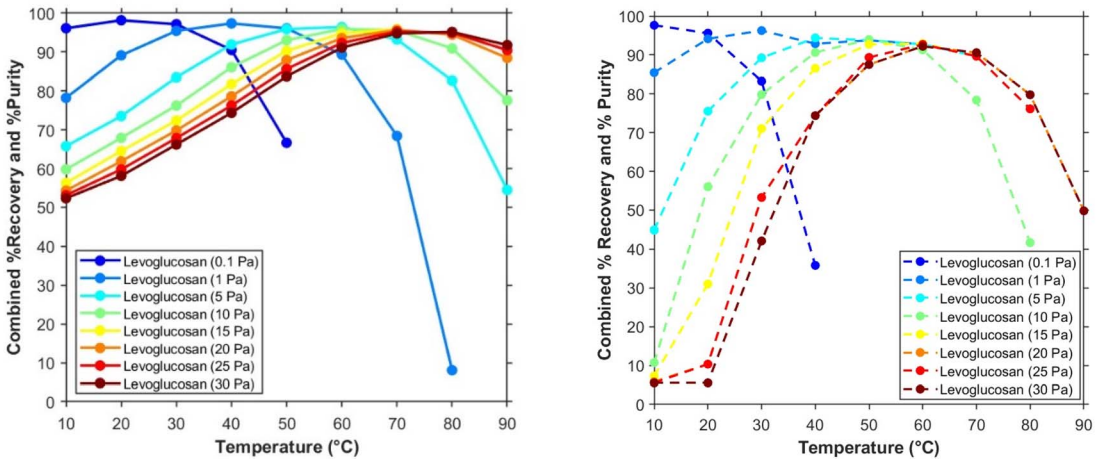

Fig. 10 The combined % recovery and % purity of the optimal levoglucosan (LVG) at different temperatures and pressures for (left) rice husk and (right) forestry residue model.

Table 7 The parameters and results for the mean free path from MD2 for the rice husk model

Compounds	Molecular weight (g mol^{-1})	Critical path (Pa)	Critical temperature (K)	Co-volume, b (m^3 mol^{-1})	Particle volume, V_p (m^3 per molecule)	Particle diameter, d (cm)
4-Vinylphenol	120.15	4.67×10^6	717.70	1.11×10^{-4}	4.60×10^{-29}	6.082
1,2-Benzenediol	110.10	7.56×10^6	766.85	7.31×10^{-5}	3.03×10^{-29}	4.607
Levoglucosan	162.14	4.80×10^6	905.70	1.36×10^{-4}	5.65×10^{-29}	4.019

Table 8 The parameters and results for the mean free path from MD2 for the forestry residue model

Compounds	Molecular weight ($g\ mol^{-1}$)	Critical path (Pa)	Critical temperature (K)	Co-volume, b ($m^3\ mol^{-1}$)	Particle volume, V_p (m^3 per molecule)	Particle diameter, d (m)
Mnapthen	142.20	4.36×10^6	784.00	1.30×10^{-4}	5.38×10^{-29}	4.68×10^{10}
p-Hydroquinone	110.11	7.56×10^6	766.85	7.31×10^{-5}	3.03×10^{-29}	3.87×10^{10}
Methyl-salicylate	152.15	4.69×10^6	709.00	1.09×10^{-4}	4.52×10^{-29}	4.42×10^{10}
Levoglucosan	162.14	4.80×10^6	905.70	1.36×10^{-4}	5.65×10^{-29}	4.76×10^{10}

Table 9 Evaporation flux and area of evaporator for both models

Molecular distillation unit	Feed ($kg\ h^{-1}$)	Vapor ($kg\ h^{-1}$)	Flux ($kg\ m^{-2}\ s$)	Area (m^2)
MD2 (rice husk model)	32 049.09	22 441.07	0.0108	574.72
MD2 (forestry residue model)	23 581.68	22 545.0	0.010	567.44

residue which was 947.2 $kg\ h^{-1}$. Therefore, more levoglucosan would be obtained from the rice husk biomass as the feed than the forestry residue.

3.4.3 Mean free path and evaporation flux. In this study, the simulations were also used to evaluate the evaporation characteristics of the molecular distillation unit for the separation of levoglucosan amongst other products of interest. Additionally, the simulations were utilized to establish the optimal process conditions. Thereafter, this was employed to determine the free mean path of the interested components and calculate the distance between the condenser and evaporator to make separation easier and more efficient.

Hence, in MD2, the mean free paths of the isolated compounds for the rice husk model were 6.082 cm, 4.607 cm, and 4.019 cm for 1,2-benzenediol, 4-vinylphenol, and levoglucosan respectively. 1,2-benzenediol had the highest mean free path, which was closely followed by 4-vinylphenol and levoglucosan. For the forestry residue, the mean free paths were 4.008 cm, 5.875 cm, 4.503 cm, and 3.882 cm for mnapthen, *p*-hydroquinone, methyl-salicylate, and levoglucosan respectively. *p*-Hydroquinone had the highest mean free path, followed by methyl-salicylate, mnapthen, and then levoglucosan. Thus, the mean free paths of the compounds decreased with an increase in pressure and molecular diameter but increased slightly with temperature. This can be attributed to their respective molecular weights, as it validates the theory of the mean free path, that the lower the molecular weight of a compound, the higher the free mean path. Thus the faster the components will get to the evaporator to be condensed.[24] Accordingly, this implies that both 1,2-benzenediol and 4-vinylphenol are in reduced amounts in the residue stream. Since they have higher mean free paths (*i.e.* they would be able to travel longer distances before collision would occur) and would easily get to the evaporator for condensation faster than their counterpart Levoglucosan.

Tables 7 and 8 below illustrate that levoglucosan had the lowest mean free path and thus makes it possible to be separated from other bio-oil components in the molecular distillation unit. Hence, it would not travel large distances before the collision with other molecules occurs, thereby settling at the bottom stream rather than at the top stream where evaporation took place. Therefore, this is affirmed since the amount of purity of the levoglucosan obtained at the optimal operating condition in this work was 99.45% for the rice husk model and 98.21% for the forestry residue model.

Consequently, the simulations performed in this work separation do validate the physical separation as seen in the literature.[24] For the Langmuir & Knudsen–Hertz evaporation theory, the primary assumption that was used to calculate the mass flux was the ideal gas law. Considering that the substances in the vapor phase were a mixture of less-than-ideal gases, the thermodynamic model employed to represent this was a cubic equation of state. Hence, it was not anticipated that the evaporator area calculated from the data would not be entirely accurate. This theory is postulated to be true as can observed from Table 9, where the area of a molecular distillation evaporator designed for 30 000–40 000 $kg\ h^{-1}$ at 70 °C is 7 m^2 and 20 000–30 000 $kg\ h^{-1}$ at 70 °C is 6.5 m^2.[24]

4 Conclusion

A process model for the rice husk and forestry residues fast pyrolysis process integrated with molecular distillation for the first time was developed in this study using ASPEN Plus V12 software. The experimental data used as input in the model and the simulation results were validated with experimental results. The yields of the pyrolysis gases and bio-oil compounds were compared between simulation and experimental data. It was observed that the simulation results are in good agreement with the experimental results. However, there was a maximum variation between the experimental and simulation results of less than 13%. It was observed that the yields of the major bio-oil compounds present in both biomasses increased with an increase in the temperature. To separate specific viable chemicals of interest, the molecular distillation unit was simulated for rice husk and forestry residue biomass. The % purity and % recovery of levoglucosan

at the optimal operating conditions of 20 °C and 0.1 Pa were 99.45% and 98.72% for the rice husk. While for the forestry residue biomass at the optimal operating conditions were 10 °C and 0.1 Pa were 98.21% and 97.41%.

The major chemicals isolated for rice husk and forestry residue biomass include levoglucosan, 1,2-benzenediol, 4-vinylphenol, mnapthen, *p*-hydroquinone, and methyl-salicylate. The mean free paths were 6.082, 4.607 cm, and 4.019 cm for 1,2-benzenediol, 4-vinylphenol, and levoglucosan respectively. For the forestry residue, the mean free paths were 4.008 cm, 5.875 cm, 4.503 cm, and 3.882 cm for mnapthen, *p*-hydroquinone, methyl-salicylate, and levoglucosan respectively. These mean free paths decreased with an increase in pressure and molecular diameter but increased slightly with temperature. The composition and separation of the compounds were compared with the differences in the molecular mean free path to justify the separation of the chemicals and hence validate the model. There is good agreement with the literature. Thereafter sensitivity analysis was performed to optimize the molecular distillation unit. The model developed in this study can be used to analyze complex reactive systems, give valuable insights into optimizing different pyrolysis parameters, and how to separate single bio-oil compounds of interest. Thus, it can be deduced that the integration of molecular distillation with fast pyrolysis can accurately be used to predict the yield, bio-oil compounds, and isolate selected chemicals and fuels for various biomass waste.

Nomenclature

d	Effective particle diameter, m
a, b	Co-volume, m^3
HHV	Higher heating value, MJ kg^{-1}
N_A	Avogadro's number, molecules mol^{-1}
λ	Mean free path, cm
P	Pressure, Pa
R	Ideal gas law, J mol^{-1} K^{-1}
T	Temperature, °C, or K
V_m	Molar volume, m^3 mol^{-1}
V_p	Volume of a particle, m^3

Data availability

The data supporting this article have been included as part of the ESI.†

Conflicts of interest

There are no conflicts to declare.

Acknowledgements

This work was supported by the Niger Delta Development Commission PhD scholarship [award number NDDC/DEHSS/2019PFGS/DEL/PHD/003] for Miss P. Iwube.

References

1 G. D. Okcu, Microalgae biodiesel production: a solution to increasing energy demands in Turkey, *Biofuels*, 2022, **13**(1), 77–93.
2 A. Demirbas, Progress and recent trends in biofuels, *Prog. Energy Combust. Sci.*, 2007, **33**(1), 1–18.
3 O. A. Ogungbenro, I. C. Okoro, A. E. Ohuabunwa, N. Okwuelu and P. Tagbo, Performance Analysis of Bio-Energy Based Power Generation System in Nigeria Using Rice Husk Feedstock, *Int. J. Energy Environ. Res.*, 2022, **10**(2), 40–56, DOI: 10.37745/ijeer.13vo10n2pp4056.
4 W. Hugo, *Bioenergy Atlas for South Africa: Synopsis Report*, Department of Science and Technology, 2016.
5 J. Ward, M. G. Rasul and M. M. K. Bhuiya, Energy recovery from biomass by fast pyrolysis, *Procedia Eng.*, 2014, **90**, 669–674.
6 X. Hu and M. Gholizadeh, Progress of the applications of bio-oil, *Renewable Sustainable Energy Rev.*, 2020, **134**, 110124, DOI: 10.1016/j.rser.2020.110124.
7 C. Stephan, M. Dicko, P. Stringari and C. Coquelet, Liquid-liquid equilibria of water + solutes (acetic acid/acetol/furfural/guaiacol/methanol/phenol/propanal) + solvents (isopropyl acetate/toluene) ternary systems for pyrolysis oil fractionation, *Fluid Phase Equilib.*, 2018, **468**, 49–57, DOI: 10.1016/j.fluid.2018.04.016.
8 F. Seifollahi, M. H. Eikani and N. Khandan, Optimization of operating conditions for lampante olive oil deacidification by short path molecular distillation: Waste valorization approach, *J. Cleaner Prod.*, 2024, **454**, 142304, DOI: 10.1016/j.jclepro.2024.142304.
9 Y. Kang, K. Wu, J. Sun, C. Liu, C. Su and F. Yi, Preparation of Kushui Rose (Rosa setate x Rosa rugosa) essential oil fractions by double molecular distillation: Aroma and biological activities, *Ind. Crops Prod.*, 2022, **175**(100), 114230, DOI: 10.1016/j.indcrop.2021.114230.
10 S. U. K. Reddy Sagili, et al., Optimization of wiped-film short path molecular distillation for recovery of cannabinoids from cannabis oil using response surface methodology, *Ind. Crops Prod.*, 2023, **195**, 116442, DOI: 10.1016/j.indcrop.2023.116442.
11 Z. Tang, Y. Zhang and Q. Guo, Catalytic hydrocracking of pyrolytic lignin to liquid fuel in supercritical ethanol, *Ind. Eng. Chem. Res.*, 2010, **49**(5), 2040–2046.
12 W. Deng, Y. Deng, W. Zhao, R. Zhang and Y. Jiang, Experimental and computer simulation of a molecular distillation process for the dehydration of tetramethylammonium hydroxide solution, *Sep. Purif. Technol.*, 2022, **288**, 120701, DOI: 10.1016/j.seppur.2022.120701.
13 O. Ketenoglu and A. Tekin, Computer simulation and experimental molecular distillation of olive pomace oil deodorizer distillate – A comparative study, *LWT*, 2018, **96**, 636–641, DOI: 10.1016/j.lwt.2018.06.015.
14 Á. M. Idárraga-Vélez, G. A. Orozco and I. D. Gil-Chaves, A systematic review of mathematical modeling for molecular

distillation technologies, *Chem. Eng. Process.*, 2023, **184**, 109289, DOI: 10.1016/j.cep.2023.109289.
15 J. Li, Y. Li and Y. Zheng, Development status and future research direction of molecular distillation technology, *Acad. J. Eng. Technol. Sci.*, 2022, **5**(8), 22–26, DOI: 10.25236/ajets.2022.050805.
16 S. Wang, High-Efficiency Separation of Bio-Oil, in *Biomass now-sustainable growth and use*, IntechOpen, 2013, ch. 16, p. 401.
17 H. S. Heo, *et al.*, Fast pyrolysis of rice husk under different reaction conditions, *J. Ind. Eng. Chem.*, 2010, **16**(1), 27–31.
18 D. L. van Schalkwyk, M. Mandegari, S. Farzad and J. F. Görgens, Techno-economic and environmental analysis of bio-oil production from forest residues *via* non-catalytic and catalytic pyrolysis processes, *Energy Convers. Manage.*, 2020, **213**, 112815.
19 A. Dutta *et al.*, *Process Design and Economics for the Conversion of Lignocellulosic Biomass to Hydrocarbon Fuels: Thermochemical Research Pathways with in Situ and Ex Situ Upgrading of Fast Pyrolysis Vapors*, Pacific Northwest National Lab.(PNNL), Richland, WA (United States), 2015.
20 D. S. Fardhyanti, A. Chafidz, B. Triwibowo, H. Prasetiawan, N. N. Cahyani and S. Andriyani, Improving the quality of bio-oil produced from rice husk pyrolysis by extraction of its phenolic compounds, *J. Bahan Alam Terbarukan*, 2020, **8**(2), 90–100.
21 J. E. Omoriyekomwan, A. Tahmasebi and J. Yu, Production of phenol-rich bio-oil during catalytic fixed-bed and microwave pyrolysis of palm kernel shell, *Bioresour. Technol.*, 2016, **207**, 188–196.
22 S. M. Walas, *Phase Equilibria in Chemical Engineering*, Butterworth-Heinemann, 2013.
23 W. A. Alexander, Particle Beam Scattering From the Vacuum–Liquid Interface, *Physical Chemistry of Gas-Liquid Interfaces*, 2018, pp. 195–243, DOI: 10.1016/B978-0-12-813641-6.00008-X.
24 S. Wang, *et al.*, Separation of bio-oil by molecular distillation, *Fuel Process. Technol.*, 2009, **90**(5), 738–745, DOI: 10.1016/j.fuproc.2009.02.005.
25 M. M. Hasan, M. G. Rasul, M. I. Jahirul and M. M. K. Khan, Modeling and process simulation of waste macadamia nutshell pyrolysis using Aspen Plus software, *Energy Rep.*, 2022, **8**, 429–437, DOI: 10.1016/j.egyr.2022.10.323.
26 P. Li, *et al.*, Bio-oil from biomass fast pyrolysis: Yields, related properties and energy consumption analysis of the pyrolysis system, *J. Cleaner Prod.*, 2021, **328**, 129613, DOI: 10.1016/J.JCLEPRO.2021.129613.
27 S. Paul and P. Mondel, Pyrolysis of forest residue for production of bio fuel, *Int. Energy J.*, 2006, **7**(3), 221–225.
28 X. Guo, S. Wang, Z. Guo, Q. Liu, Z. Luo and K. Cen, Pyrolysis characteristics of bio-oil fractions separated by molecular distillation, *Appl. Energy*, 2010, **87**(9), 2892–2898, DOI: 10.1016/j.apenergy.2009.10.004.
29 Q. Bu, *et al.*, Production of phenols and biofuels by catalytic microwave pyrolysis of lignocellulosic biomass, *Bioresour. Technol.*, 2012, **108**, 274–279, DOI: 10.1016/J.BIORTECH.2011.12.125.
30 I. G. Hakeem, *et al.*, Research progress on levoglucosan production *via* pyrolysis of lignocellulosic biomass and its effective recovery from bio-oil, *J. Environ. Chem. Eng.*, 2021, **9**(4), 105614, DOI: 10.1016/J.JECE.2021.105614.
31 D. Zhang, Y. Fan, A. Zheng, Z. Zhao, F. Wang and H. Li, Maximizing Anhydrosugar Production from Fast Pyrolysis of Eucalyptus Using Sulfuric Acid as an Ash Catalyst Inhibitor, *Catalysts*, 2018, **8**(12), 609, DOI: 10.3390/catal8120609.
32 Y. Fan, D. Zhang, A. Zheng, Z. Zhao, H. Li and T. Yang, Selective production of anhydrosugars and furfural from fast pyrolysis of corncobs using sulfuric acid as an inhibitor and catalyst, *Chem. Eng. J.*, 2019, **358**, 743–751, DOI: 10.1016/J.CEJ.2018.10.014.
33 M. L. Nieva, M. A. Volpe and E. L. Moyano, Catalytic and catalytic free process for cellulose conversion: fast pyrolysis and microwave induced pyrolysis studies, *Cellulose*, 2015, **22**(1), 215–228, DOI: 10.1007/s10570-014-0484-z.
34 J. Wang, Q. Wei, J. Zheng and M. Zhu, Effect of pyrolysis conditions on levoglucosan yield from cotton straw and optimization of levoglucosan extraction from bio-oil, *J. Anal. Appl. Pyrolysis*, 2016, **122**, 294–303, DOI: 10.1016/J.JAAP.2016.09.013.
35 G. F. David, O. R. Justo, V. H. Perez and M. Garcia-Perez, Thermochemical conversion of sugarcane bagasse by fast pyrolysis: High yield of levoglucosan production, *J. Anal. Appl. Pyrolysis*, 2018, **133**, 246–253, DOI: 10.1016/J.JAAP.2018.03.004.
36 M. R. Rover, P. A. Johnston, L. E. Whitmer, R. G. Smith and R. C. Brown, The effect of pyrolysis temperature on recovery of bio-oil as distinctive stage fractions, *J. Anal. Appl. Pyrolysis*, 2014, **105**, 262–268, DOI: 10.1016/J.JAAP.2013.11.012.
37 Y. Mei, S. Zhang, H. Wang, S. Jing, T. Hou and S. Pang, Low-Temperature Deoxidization of Lignin and Its Impact on Liquid Products from Pyrolysis, *Energy Fuels*, 2020, **34**(3), 3422–3428, DOI: 10.1021/acs.energyfuels.0c00202.
38 H. S. Choi and D. Meier, Fast pyrolysis of Kraft lignin - Vapor cracking over various fixed-bed catalysts, *J. Anal. Appl. Pyrolysis*, 2013, **100**, 207–212, DOI: 10.1016/j.jaap.2012.12.025.
39 F. Allais, Total syntheses and production pathways of levoglucosenone, a highly valuable chiral chemical platform for the chemical industry, *Curr. Opin. Green Sustainable Chem.*, 2023, **40**, 100744, DOI: 10.1016/j.cogsc.2022.100744.
40 M. R. Rover, A. Aui, M. M. Wright, R. G. Smith and R. C. Brown, Production and purification of crystallized levoglucosan from pyrolysis of lignocellulosic biomass, *Green Chem.*, 2019, **21**(21), 5980–5989, DOI: 10.1039/c9gc02461a.
41 G. Lyu, S. Wu and H. Zhang, Estimation and comparison of bio-oil components from different pyrolysis conditions, *Front. Energy Res.*, 2015, **3**, 1–11, DOI: 10.3389/fenrg.2015.00028.
42 A. Komesu, J. A. Rocha de Oliveira, M. R. W. Maciel and R. Maciel Filho, Simulation of Molecular Distillation

Process for Lactic Acid, *J. Chem. Chem. Eng.*, 2016, **10**(5), 230–234, DOI: 10.17265/1934-7375/2016.05.005.

43 H. Zhang, X. Meng, C. Liu, Y. Wang and R. Xiao, Selective low-temperature pyrolysis of microcrystalline cellulose to produce levoglucosan and levoglucosenone in a fixed bed reactor, *Fuel Process. Technol.*, 2017, **167**, 484–490, DOI: 10.1016/J.FUPROC.2017.08.007.

44 A. Zheng, *et al.*, Toward Fast Pyrolysis-Based Biorefinery: Selective Production of Platform Chemicals from Biomass by Organosolv Fractionation Coupled with Fast Pyrolysis, *ACS Sustain. Chem. Eng.*, 2017, **5**(8), 6507–6516, DOI: 10.1021/acssuschemeng.7b00622.